

FEATURE ARTICLE

Block-Localized Wavefunction (BLW) Method at the Density Functional Theory (DFT) Level

Yirong Mo,* Lingchun Song, and Yuchun Lin

Department of Chemistry, Western Michigan University, Kalamazoo, Michigan 49008

Received: March 27, 2007; In Final Form: May 9, 2007

The block-localized wavefunction (BLW) approach is an ab initio valence bond (VB) method incorporating the efficiency of molecular orbital (MO) theory. It can generate the wavefunction for a resonance structure or diabatic state self-consistently by partitioning the overall electrons and primitive orbitals into several subgroups and expanding each block-localized molecular orbital in only one subspace. Although block-localized molecular orbitals in the same subspace are constrained to be orthogonal (a feature of MO theory), orbitals between different subspaces are generally nonorthogonal (a feature of VB theory). The BLW method is particularly useful in the quantification of the electron delocalization (resonance) effect within a molecule and the charge-transfer effect between molecules. In this paper, we extend the BLW method to the density functional theory (DFT) level and implement the BLW-DFT method to the quantum mechanical software GAMESS. Test applications to the π conjugation in the planar allyl radical and ions with the basis sets of 6-31G(d), 6-31+G(d), 6-311+G(d,p), and cc-pVTZ show that the basis set dependency is insignificant. In addition, the BLW-DFT method can also be used to elucidate the nature of intermolecular interactions. Examples of π -cation interactions and solute-solvent interactions will be presented and discussed. By expressing each diabatic state with one BLW, the BLW method can be further used to study chemical reactions and electron-transfer processes whose potential energy surfaces are typically described by two or more diabatic states.

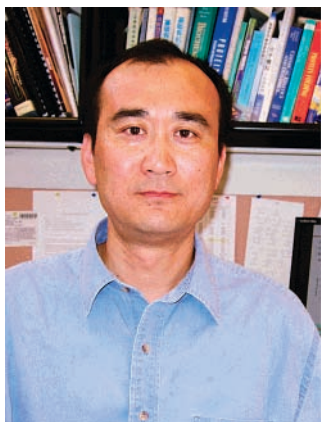
1. Introduction

Often our contemporary chemical models and thinking are broadly dependent on the Lewis concept of electron pair bonding proposed more than 90 years ago,^{1,2} which was later confirmed by Heitler and London in the case of the hydrogen molecule³ and generally developed to valence bond (VB) theory by Slater and Pauling.^{4–6} Within the framework of VB theory, a conjugated molecule or a chemical reaction (adiabatic state) can be normally described by a few resonance structures or processes (diabatic states) that are characterized by localized chemical bonds. Alternatively, molecular orbital (MO) theory assigns electrons to the canonical MOs that are linear combinations of atomic orbitals. In other words, MOs are delocalized over the whole molecular system. Although canonical MOs can be transformed to nonoptimal localized MOs that more or less correspond to electron pair bonds by ad hoc localizing algorithms,⁷ a long-standing challenge in modern theoretical chemistry has been on how to accommodate the conventional VB theory and concepts into the ab initio paradigm, which is now overwhelmingly dominated by the MO-based methods. For instance, the quantitative study of the electron delocalization (conjugation) within a molecule or electron-transfer effect between molecules requires an unambiguous definition of the reference diabatic state where the electron delocalization or transfer is quenched. Due to the delocalization nature of MOs,

it is difficult if not impossible to uniquely define and self-consistently optimize the wavefunction for a specific diabatic state within MO-based methods. In contrast, VB theory is established on resonance structures (or diabatic states), and each diabatic state can be concisely represented by a Heitler-London-Slater-Pauling (HLSP) function.⁴ Computationally, the most remarkable difference between the VB and MO theories lies in the nonorthogonality of orbitals in the former. Although the nonorthogonality centers on many chemical models and is in agreement with the fundamental assumption that chemical bonds originate from the overlap of bonding orbitals, it leads to the so-called $N!$ problem (N refers to the number of electrons in a system), which indicates that all terms are non-negligible in the evaluation of Hamiltonian and overlap matrix elements. In the MO theory, however, the orthogonality constraint of MOs greatly reduces the computational complexity by zeroing most of the terms and is largely responsible for the popularity of the MO methods in the current computational chemistry field.

During the past two decades, VB theory has regained its momentum and enjoyed a renaissance to some extent with the completion and releasing of a few modern ab initio VB computational codes,^{2,8–11} including the Xiamen VB (XMVB) package.^{12,13} This spin-free ab initio VB code is based on a novel algorithm called paired-permanent approach and contains the capabilities of VB self-consistent field (VBSCF), breathing orbital VB (BOVB), and VB configuration interaction (VBCI) computations. Although the high computational cost still limits

* Corresponding author. Tel: 269-387-2916, 269-387-2909. E-mail: yirong.mo@wmich.edu.



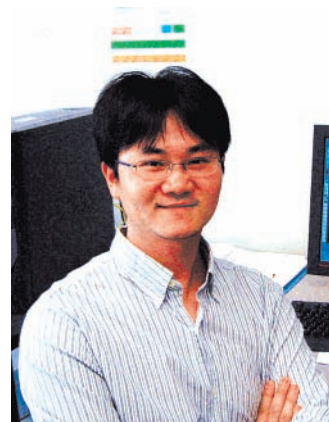
Yirong Mo received his B.S. in physical chemistry in 1986 and Ph.D. in quantum chemistry in 1992 from Xiamen University (China). His Ph.D. work involves the development and applications of the ab initio valence bond theory with Professor Qianer Zhang. He was a DAAD Visiting Fellow with Professor Paul Schleyer at the University of Erlangen-Nürnberg and a Humboldt Research Fellow with Professor Sigrid Peyerimhoff at Bonn University in Germany in 1996–1997. During this period, he started to develop the BLW method. From the end of 1998 to the middle of 2001, he worked with Professor Jiali Gao at the State University of New York at Buffalo and University of Minnesota as a research associate on the development of the combined QM(MOVB)/MM method and molecular dynamics simulations of enzymatic catalysis. After working as a Computational Biochemist at Xencor for 1 year, he moved to the Western Michigan University in the August of 2002 where he is presently an Associate Professor of Chemistry. He is also an Adjunct Professor at Xiamen University. His research interests include the electron-transfer theory and the modeling and engineering of biological systems.



Lingchun Song obtained his B.S. (1997) and his Ph.D. (2002) in physical chemistry from Xiamen University, China. After graduation, he remained at Xiamen University and was promoted to Associate Professor in 2005. He joined Professor Mo's group at Western Michigan University as a Visiting Scientist in 2006. Currently he is doing his postdoctoral research in Professor Jiali Gao's group at the University of Minnesota. His research interests include ab initio and semiempirical valence bond theory, inter- and intramolecular interaction, and QM/MM methods for simulations of proteins.

the application of the ab initio VB methods to small systems, the impact of this development on the reformation of our chemical knowledge is significant and diverse.^{11,14} Compared with MO theory, VB theory provides a concise description of multireference character and an intuitive model for a chemical reaction and its potential energy surface.

Apart from the recent advance in ab initio VB methods, numerous empirical or semiempirical VB approaches have been proposed and applied to the study and reinterpretation of a wide range of structural and mechanistic problems in chemistry.^{10,15–22} Notably, empirical VB (EVB) approaches use the VB picture of chemical bonding to describe the changes of bonding in the



Yuchun Lin received a B.S. degree in Chemistry and an M.S. in quantum chemistry from Xiamen University at 2000 and 2003, respectively. He then joined a Ph.D. program at Western Michigan University under the supervision of Professor Yirong Mo. His research interests are in the areas of developing novel approaches to model and engineer pesticide-degrading enzymes with higher activity and diversity, elucidating the mechanism of ion or gas membrane proteins, and applying the BLW method to the study of inter- and intramolecular electron transfer.

process of a chemical reaction from reactants to products and typically involves two resonance (diabatic) states (multistate EVB or multiconfiguration MM approaches are also available^{19,20,23}), namely one reactant state A and one product state B. Whereas the ground state potential results from the mixture of both diabatic states, the potential function associated with each diabatic state is expressed in terms of molecular mechanical (MM) force fields. The key of various EVB approaches is the off diagonal matrix element H_{AB} (S_{AB} is assumed zero), which is often simply approximated with an exponential function,^{15,16} or a generalized Gaussian form^{17,23} or its improved forms.^{19,21} In fact, the computation of H_{AB} also centers on the electron-transfer theory because it is directly related to the electron-transfer rate.^{24,25} In EVB approaches, H_{AB} is calibrated to fit the resulting potential energy surface to either the experimental or high level ab initio data. Moreover, it is often assumed that changes of H_{AB} due to the environment (e.g., from solution to protein) are negligible. This ad hoc key EVB assumption is validated for the test case of S_N2 reactions using the frozen density functional theory (DFT) and the constrained DFT approaches recently.²⁶ Numerous applications have distinctively demonstrated the importance of the VB approaches in gaining new insights into molecular structures, properties, and reactivity in both gaseous and condensed phases, which are supplementary to those obtained from MO computations. Even for complicated enzyme-catalyzed reactions, simple VB concepts and ideas have shown their distinctive values.^{16,27} However, the further utilization of the VB ideas at the empirical and semiempirical levels should be carefully scrutinized by benchmark ab initio VB computations. It is thus highly desirable to develop ab initio VB-like approaches with high computational efficiency.

A promising strategy is to combine the advantage of MO and VB theories. One successful example in this regard is Goddard's generalized VB (GVB) method,²⁸ which retains the VB form for one or a few focused bonds (perfect-pairs) but accommodates the remaining electrons with orthogonal and doubly occupied MO's. Recently, we proposed the block-localized wavefunction (BLW) method at the Hartree–Fock (HF) level which is as efficient as the conventional HF method.^{29–34} Instead of allowing all MOs to be a combination of all atomic orbitals in MO theory, this BLW method defines the wavefunction for a diabatic state by limiting the expansion

of each MO (called block-localized MO) to a predefined subspace. As a consequence, block-localized MOs belonging to different subspaces are generally nonorthogonal. In such a way, the BLW method preserves the characteristics and advantages of both the VB and MO theories. Significantly, the BLWs for diabatic states are optimized self-consistently, and the adiabatic state is a combination of a few (usually two or three) diabatic state wavefunctions. Although the usefulness of the BLW method has been demonstrated by a range of applications and the comparison between the BLW and modern ab initio VB calculations where electron correlations are taken into account confirms the reliability of the BLW method,^{32,33,35} we note that the current BLW method is implemented at the HF level where electron correlation effects are not considered.

Kohn–Sham DFT has a self-consistent procedure identical to the HF method except that the HF exchange potential is replaced by a DFT exchange–correlation (XC) potential. But significantly, DFT includes dynamical electron correlation and some static correlation.³⁶ Thus, the extension of the BLW method to the DFT level is highly expected and feasible. In this paper, we will describe our recent development and implementation of the BLW–DFT method for systems of either closed or open shells. The developed computational codes have been ported to the most recent version of GAMESS software.³⁷ Test calculations will also be presented and discussed.

2. Methodology

2.1. Ab Initio Valence Bond (VB) Theory. In VB theory, a resonance structure is constructed with chemical bonds each of which concerns only two atoms and is thus strictly localized. For a system of $N = 2n + 2S$ electrons (n is the number of electron pairs and S is the spin quantum number), each resonance structure can be uniquely expressed by a HLSP function as

$$\Psi_K = M_K \hat{A}(\varphi_{1,2} \varphi_{3,4} \cdots \varphi_{2n-1,2n} \phi_{2n+1} \alpha(2n+1) \cdots \phi_N \alpha(N)) \quad (1)$$

where M_K is the normalization constant, \hat{A} is the antisymmetrizer, and $\varphi_{2i-1,2i}$ is a bond function corresponding to the chemical bond between orbitals ϕ_{2i-1} and ϕ_{2i} (or a lone pair if $\phi_{2i-1} = \phi_{2i}$)

$$\varphi_{2i-1,2i} = \hat{A}\{\phi_{2i-1} \phi_{2i} [\alpha(2i-1) \beta(2i) - \beta(2i-1) \alpha(2i)]\} \quad (2)$$

In eq 1 there are $2S$ singly occupied orbitals from ϕ_{2n+1} to ϕ_N . As each bond function (eq 2) can be expanded into two Slater determinants, a HLSP comprises of 2^n Slater determinants. The overall many-electron wavefunction for an adiabatic (ground or excited) state is consequently a linear combination of important VB functions⁶

$$\Psi = \sum_K C_K \Psi_K \quad (3)$$

where the coefficients $\{C_K\}$ are determined by solving the secular equation $\mathbf{HC} = \mathbf{ESC}$. But the evaluation of the Hamiltonian and overlap matrix elements between VB functions remains a challenge (the so-called “ $N!$ problem”) for ab initio VB methods due to the nonorthogonality of VB orbitals $\{\phi\}$. For instance, the Hamiltonian matrix element based on determinants is expressed as

$$\langle D_i | H | D_j \rangle = \sum_{r,s} f_{rs} D(S_r^s) + \sum_{r<u,s<t} (g_{rs,ut} - g_{rs,tu}) D(S_{ru}^{st}) \quad (4)$$

where f_{rs} and $g_{rs,ut}$ are one-electron and two-electron integrals

respectively, and $D(S_r^s)$ and $D(S_{ru}^{st})$ are the first and the second-order cofactors of the overlap matrix between the two VB determinants, respectively. Over the years, several groups have developed efficient algorithms to simplify the computations of the Hamiltonian and overlap matrix elements.⁹ Among them, the XMVB code adopts the novel paired-permanent determinant (PPD) algorithm.^{12,38} For a $N \times N$ matrix $i, j = 1, 2, \dots, N$, a PPD is defined as

$$\text{PPD}(A) = \sum_{P \in S_N} D_{11}^{[1]}(P) a_{1p_1} a_{2p_2} \cdots a_{N-1,p_{N-1}} a_{N,p_N} \quad (5)$$

where P is a permutation and $D_{11}^{[1]}(P)$ is the first diagonal matrix element associated with the permutation P for the standard Young–Yamanouchi orthogonal irreducible representation $[\lambda]$. The computation of a PPD function is performed by a procedure similar to the Laplace expansion algorithm for determinants. A N -order PPD can be reduced to PPD’s of order $(N-2)$, $(N-4)$, etc., and finally to 2-order PPD’s for close shell systems. In the routine of a PPD expansion, there are many redundant sub-PPDs. Thus, all required sub-PPDs are computed in advance, labeled by indices, and stored in an external dataset file which can be loaded when it is needed.

2.2. Bond Functions and Generalized Valence Bond (GVB) Method. One dramatic way to boost the computational efficiency of VB methods is the replacement of the bond function shown in eq 2 with a doubly occupied MO-like localized orbital

$$\varphi_{2i-1,2i} = \hat{A}\{\phi'_i \phi'_i [\alpha(2i-1) \beta(2i)]\} \quad (6)$$

where ϕ'_i is usually localized over the two bonding atoms and nonorthogonal with others.^{39,40} As such, the VB wavefunction eq 1 is reduced to a single Slater determinant. Bond functions are particularly suitable for the discussion of intramolecular electron delocalization. For example, Sover et al. examined the barrier potential to internal rotation in ethane with this kind of bond-orbital wavefunctions and concluded that the dominant contribution to the barrier is the repulsion between C–H bond orbitals.⁴⁰ This form of wavefunction can also be used to study the effects of conjugation and hyperconjugation by substituting the π MO’s in the HF wavefunction with ethylene π MO’s derived from calculations of ethene with the same basis set.^{41,42} Apparently, the further introduction of orthogonality and delocalization over the whole system for orbitals $\{\phi'_i\}$ leads to the much familiar HF wavefunction.

The very successful GVB method can be regarded as the hybrid use of eqs 2 and 6 in Ψ_K ,²⁸ where the focused perfect-pairs are expressed in VB form (eq 2), but the rest electrons are put into orthogonal and doubly occupied MO’s in the form of eq 6. The introduction of the strong orthogonality constraint between VB orbitals and MO’s significantly reduces the computational demand for GVB calculations. The GVB method is particularly advantageous for the study of excited states and photodissociation pathways which cannot be well described with a single-determinant HF wavefunction.

2.3. Block-Localized Wavefunction (BLW) Method. A further simplification of the VB wavefunction is the use of group functions instead of bond functions by allowing the doubly occupied bond function (eq 6) to partially delocalize over a fragment of the system instead of only two bonding atoms. This kind of combination of the VB and MO theories has the remarkable advantage of using the least number of diabatic states to describe an overall chemical reaction process. For instance, in the Marcus–Hush model for a donor–acceptor system,^{24,43} the electron-transfer (ET) process is normally described by two

electron-localized diabatic states, namely one pre-ET and one post-ET states. Because the focus is the electron transfer from the donor to the acceptor, usually the electron delocalization within the donor or acceptor per se is not our concern and thus it was better to use one concise wavefunction instead of several VB wavefunctions for the donor or acceptor to simplify both the numerical computations and conceptual picture. But in terms of the whole donor–acceptor complex, either the donor or acceptor is only a fragment, and both the pre-ET and one post-ET states need to be defined individually following the VB concepts. Putting the above considerations together, recently we generalized the idea of localized bond functions and proposed the BLW method.^{29–34} In the BLW approach it is assumed that the overall electrons and primitive basis functions in a system are partitioned into several physically defined subgroups, in line with the conventional VB ideas. The *i*th subspace consists of $\{\chi_{i\mu}, \mu = 1, 2, \dots, m_i\}$ basis functions and accommodates n_i electrons. Clearly, for a resonance structure every two electrons form a subspace. However, we extend the definition of resonance structures to diabatic states and allow a subspace to have any number of electrons. The block-localized MOs for the *i*th subspace $\{\varphi_{ij}, j = 1, 2, \dots, m_i\}$ are expanded with m_i basis functions $\{\chi_{i\mu}\}$

$$\varphi_{ij} = \sum_{\mu=1}^{m_i} C_{ij\mu} \chi_{i\mu} \quad (7)$$

Subsequently, the BLW is defined using a Slater determinant and in the case of $S = 0$, it is

$$\Psi_K^{\text{BLW}} = M_K (N!)^{-1/2} \det[\varphi_{11}^2 \varphi_{12}^2 \dots \varphi_{1(n_1/2)}^2 \varphi_{21}^2 \dots \varphi_{i1}^2 \dots \varphi_{i(n_i/2)}^2 \dots \varphi_{k(n_k/2)}^2] \quad (8)$$

Orbitals in the same subspace are subject to the orthogonality constraint, but orbitals belonging to different subspaces are nonorthogonal in general. Thus, the BLW method combines the characteristics of both the MO and VB theories. For the example of a S_N2 reaction $A + BC \rightarrow AB + C$, we can define two BLWs for the reactant and product states as

$$\Psi_r^{\text{BLW}} = M_r \hat{A}[\Phi(A) \Phi(BC)] \quad (9a)$$

$$\Psi_p^{\text{BLW}} = M_p \hat{A}[\Phi(AB) \Phi(C)] \quad (9b)$$

where A and BC form two blocks (Φ is a successive product of all occupied block-localized MOs in a block) in the reactant state Ψ_r^{BLW} and the product state Ψ_p^{BLW} consists of AB and C blocks. By defining the electron density matrix

$$\mathbf{D} = \mathbf{C}(\mathbf{C}^+ \mathbf{S} \mathbf{C})^{-1} \mathbf{C}^+ \quad (10)$$

where \mathbf{S} is the overlap matrix of the basis functions. The energy of the BLW can be determined as

$$E^{\text{BLW}} = \langle \Psi^{\text{BLW}} | H | \Psi^{\text{BLW}} \rangle = \sum_{\mu=1}^m \sum_{\nu=1}^m d_{\mu\nu} h_{\mu\nu} + \sum_{\mu=1}^m \sum_{\nu=1}^m d_{\mu\nu} F_{\mu\nu} \quad (11)$$

where $h_{\mu\nu}$ and $F_{\mu\nu}$ are elements of the usual one-electron and the Fock matrices, and $d_{\mu\nu}$ is an element of \mathbf{D} .

The self-consistent optimization of orbitals in the BLW method is the key to distinguish it from other post-SCF localization methods⁷ and can be accomplished using successive Jacobi rotation²⁹ or the algorithm by Gianinetta et al.^{44,45} The latter generates coupled Roothaan-like equations and each equation corresponds to a block. For the example of two blocks *a* and *b*, the coefficient matrix takes the diagonal form

$$\mathbf{C} = \begin{pmatrix} \mathbf{C}_a & 0 \\ 0 & \mathbf{C}_b \end{pmatrix} \quad (12)$$

where \mathbf{C}_a and \mathbf{C}_b are submatrixes. The overlap matrix \mathbf{S} can also be partitioned as

$$\mathbf{S} = \begin{pmatrix} \mathbf{S}_{aa} & \mathbf{S}_{ab} \\ \mathbf{S}_{ba} & \mathbf{S}_{bb} \end{pmatrix} \quad (13)$$

The effective overlap matrix \mathbf{S}' , and effective Fock matrix \mathbf{F}' for block *a* are defined as

$$\mathbf{S}'_a = \mathbf{S}_{aa} - \mathbf{S}_{ab} \mathbf{D}_b \mathbf{S}_{ba} \quad (14a)$$

$$\mathbf{F}'_a = (\mathbf{1}_a | - \mathbf{S}_{ab} \mathbf{D}_b) \mathbf{F} \begin{pmatrix} \mathbf{1}_a \\ -\mathbf{D}_b \mathbf{S}_{ba} \end{pmatrix} \quad (14b)$$

The general stationary condition for each block, e.g., for *a*, is

$$\begin{cases} \mathbf{F}'_a \mathbf{C}_a = \mathbf{F}'_a \mathbf{C}_a \mathbf{L}_a \\ \mathbf{C}_a^+ \mathbf{S}'_a \mathbf{C}_a = \mathbf{1}_a \end{cases} \quad (15)$$

More details on the Gianinetta et al.'s algorithm can be found in their original literature.^{44,45} Obviously, it is straightforward to extend the above two-block algorithm to cases of any number of blocks, as eq 15 can be solved sequentially for each block and the rest is regarded as one block. Furthermore, the first derivative of the energy with respect to nuclear coordinates $\{q_i\}$ directly takes the form in conventional HF theory⁴⁵

$$\frac{\partial E^{\text{BLW}}}{\partial q_i} = 2 \sum_{\mu\nu}^m d_{\mu\nu} \frac{\partial h_{\mu\nu}}{\partial q_i} + \sum_{\mu\nu\rho\sigma}^m [2d_{\mu\nu} d_{\rho\sigma} - d_{\mu\rho} d_{\nu\sigma}] \frac{\partial(\mu\nu|\rho\sigma)}{\partial q_i} - 2 \sum_{\mu\nu}^m W_{\mu\nu} \frac{\partial S_{\mu\nu}}{\partial q_i} \quad (16)$$

where $W_{\mu\nu}$ is a Lagrangian variable. With the first derivatives derived analytically, the second derivatives can be computed numerically.

We have written an independent BLW code at the HF level with high efficiency, and numerous applications endorse its usefulness. For instances, we have studied the charge transfer in the prototype of donor–acceptor complexes BH_3NH_3 ,³⁵ probed the nature of the ethane rotation barrier⁴⁶ and the cation– π interactions in δ -opioid receptor binding,⁴⁷ proposed an energetic measure of aromaticity and antiaromaticity based on the Pauling–Wheland resonance energies,³³ and analyzed the charge transfer between solute and solvent with up to 1202 basis functions.⁴⁸

However, we should point out that as VB theory focuses on individual atoms and atomic orbitals, ab initio VB methods and the BLW method may not work well if the basis functions lose atomic characteristics, e.g., when a complete basis on a single center for a molecular system is used. As a matter of fact, this unphysical basis set artifact complicates not only ab initio VB methods but also MO-based analyses on atomic properties in molecules, and in reality we are using basis functions optimized

for individual atoms. Thus, the BLW method is applicable with regular basis sets and with the currently popular basis sets from 6-31G(d) to 6-311+G(d,p) and cc-pVTZ, our tests show that the basis set dependence is generally trivial for the BLW method.^{29,33,49,50}

2.4. BLW Method at the Density Functional Theory (DFT) Level. Due to the low computational costs and incorporation of (at least partial) electron correlation, DFT methods provide a sound basis for the development of computational strategies for studying potential energy surfaces, dynamics, various response functions and spectroscopy, excited states, and many more.⁵¹ Although there are several known deficiencies in DFT, e.g., DFT is less accurate for weak interactions (nonbonded interactions) and π -bonded systems, significant and persistent efforts have been put forth to develop new functionals, particularly the critical exchange and correlation functional.⁵² For the sake of simplicity, approximate dispersion corrections, e.g., a C_6/r^{-6} term, can be added to DFT calculations directly.⁵³

In DFT, the self-consistent Kohn–Sham (KS) procedure is strictly analogous to the Hartree–Fock–Roothaan SCF procedure, except that the HF exchange potential is replaced by a DFT exchange–correlation (XC) potential. And the orbital equations of DFT have the same forms as those in HF theory except with a different Fock matrix

$$\mathbf{F}^\alpha = \mathbf{H} + \mathbf{J} + \mathbf{F}^{\text{XC}\alpha} \quad (17)$$

where \mathbf{H} is the one-electron Hamiltonian matrix and \mathbf{J} is the Coulomb matrix. The elements of α exchange–correlation matrix $\mathbf{F}^{\text{XC}\alpha}$ can be evaluated by a one-electron integral involving the local electron spin densities (LSD methods), or by an integral involving electron densities and their gradients (GGA methods). Thus, it is fairly straightforward to implement the BLW idea into DFT as long as we keep all the equations (eqs 7–16) unchanged except that the Fock matrix therein is replaced by a DFT one ($\mathbf{F}^{\text{XC}\alpha}$). Recently, we extended the BLW method to the DFT level by adopting the block-localized orbitals in the KS-DFT procedure, and the implementation of the BLW-DFT method consists of the following steps:

- (i) Construct the DFT Fock matrix and calculate the DFT energy.
- (ii) Construct the effective Fock and overlap matrices for each block.
- (iii) Solve the generalized secular equations and subsequently form the new coefficient and density matrix.
- (iv) Check the variation of the density matrix. Go back to the first step if convergence is not reached; otherwise, print out the final outcome and compute various properties.

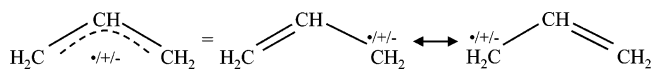
Because achieving a self-consistent field with DFT is usually more difficult than with the normal HF method, Pulay's DIIS technique is used to update the Fock matrix and accelerate the convergence.⁵⁴ The fluctuation of density matrix in the process of iteration will be taken as the error vector. Fortunately, the present version of GAMESS has the capability of performing DFT calculations;³⁷ thus we used GAMESS as a platform to implement the BLW-DFT method.

The formulation of the BLW method for open-shell systems is quite similar to eqs 7–16 where the doubly occupied orbitals are replaced with singly occupied spin–orbitals. In other words, we replace the Fock matrix with the α and β Fock matrices in the restricted or restricted open-shell self-consistent equations. The current version of BLW-DFT works for both closed-shell and open-shell systems.

3. Test Calculations with the BLW-DFT Code

The BLW method at both the HF and DFT levels has been implemented and ported to the general ab initio quantum chemistry package GAMESS software³⁷ and the code has the geometry optimization capabilities.³¹ The BLW method can not only evaluate the Pauling–Wheland resonance energy in conjugated systems^{29,33} but also explore the nature of intermolecular interactions and decompose the interaction energy in terms of Heitler–London, polarization, and electron-transfer energy terms, where the Heitler–London energy term can be further decomposed to electrostatic and Pauli exchange interactions.^{30,35,48,50,55} In the following we will present a few preliminary applications of the BLW-DFT code to the resonance in the allyl radical and its cation and anion, the nature of π -cation interaction between a few cations and benzene, and the charge transfer between solute and solvent with the supermolecular models of a positively charged ammonium and its methyl substitutes methylamines $\text{Me}_n\text{NH}_{4-n}^+$ ($n = 0-3$) plus a few water molecules surrounding each cation.

3.1. Conjugation in Allyl Radical and Ions. The allyl systems (radical, cation, and anion) are classical examples to illustrate the resonance theory as well as the Hückel MO theory, and described with two resonance structures as



These allyl systems are considered to be stabilized by electron delocalization. According to the original definition of Pauling and Wheland in VB theory,^{5,6,56} the magnitude of resonance is measured by the resonance energy (RE), which is “obtained by subtracting the actual energy of the molecule in question from that of the most stable contributing structure.”⁵⁶ Within the MO theory, however, approximations must be taken to quantify the resonance effect. For instance, if the rotation of a part of a system can deactivate the conjugation effect over the rotated bond, the subsequent rotation barrier can be used to approximate the resonance stabilization energy.⁵⁷ But the involvement of other factors such as hyperconjugation effect, steric effect, etc. in the rotation process may severely complicate the interpretation of the rotation barrier.^{42,49} As a matter of fact, the strength of resonance stabilization in the allyl systems has been controversial.^{22,32,58–61} Wiberg et al. studied the rotation barriers in allyl ions in terms of electronic delocalization and electrostatic energies and concluded that the resonance stabilization is negligible in the anion but significant in the cation,⁵⁸ and Gobbi and Frenking argued that the conjugative contribution to the resonance stabilization is comparable in magnitude in the three allyl systems.⁵⁹ Our ab initio VB studies showed that the allyl cation and anion possess comparable resonance stabilization but the radical has only half of that strength.⁶⁰

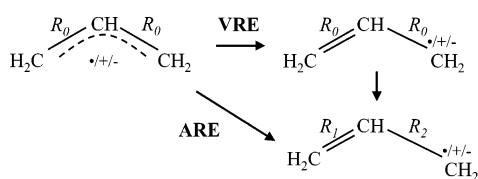
Here we performed both the regular DFT and BLW-DFT calculations to derive the delocalized and localized (the most stable resonance) structures with the basis sets of 6-31G(d), 6-31+G(d), 6-311+G(d,p) and cc-pVTZ. On the basis of the geometries employed, two types of resonance energies are defined (Scheme 1). One is the vertical resonance energy (VRE) which is the energy difference between the optimal delocalized state and its most stable resonance contributor at the same geometry. The other is called adiabatic resonance energy (ARE) which is the energy difference between the optimal delocalized state and the optimal resonance structure; i.e., both geometries are relaxed. The difference between VRE and ARE reflects the compression energy for the σ -frame. Results are compiled in Table 1.

TABLE 1: Optimal Carbon–Carbon Bond Lengths (Å) and Resonance Energies (kcal/mol) in Allyl Systems at the DFT Level

| allyl | basis set | delocalized structure | localized structure | | VRE | ARE |
|---------|--------------|-----------------------|---------------------|-------|------|------|
| | | R_0 | R_1 | R_2 | | |
| radical | 6-31G(d) | 1.384 | 1.330 | 1.514 | 31.8 | 22.7 |
| | 6-31+G(d) | 1.387 | 1.333 | 1.519 | 32.7 | 23.5 |
| | 6-311+G(d,p) | 1.382 | 1.327 | 1.519 | 33.1 | 23.6 |
| | cc-pVTZ | 1.378 | 1.323 | 1.509 | 32.1 | 23.2 |
| cation | 6-31G(d) | 1.385 | 1.333 | 1.501 | 57.6 | 50.7 |
| | 6-31+G(d) | 1.385 | 1.335 | 1.502 | 56.3 | 49.4 |
| | 6-311+G(d,p) | 1.381 | 1.330 | 1.498 | 55.6 | 48.8 |
| | cc-pVTZ | 1.377 | 1.328 | 1.472 | 51.1 | 46.3 |
| anion | 6-31G(d) | 1.394 | 1.341 | 1.507 | 53.0 | 46.1 |
| | 6-31+G(d) | 1.399 | 1.340 | 1.538 | 51.5 | 42.4 |
| | 6-311+G(d,p) | 1.395 | 1.335 | 1.537 | 51.4 | 41.9 |
| | cc-pVTZ | 1.390 | 1.336 | 1.508 | 48.5 | 41.8 |

Although the allyl systems show insignificant basis set dependence in terms of both the geometries and resonance energies, a general trend is that cc-pVTZ tends to slightly shrink bonds in both DFT and BLW-DFT optimizations, particularly for the single bonds in the allyl ions. In addition, for the allyl anion the 6-31G(d) basis set results in a shorter single bond (R_2) and higher resonance energies than other basis sets. This indicates the importance of diffuse functions for anions as well recognized. As expected, the charge localization in the optimal localized structures makes the double bonds converge to the ethylene double bond, and the optimal C sp^2 –C sp^2 single bond length in the allyl radical is consistent with the computations of other neutral polyenes and benzene.^{31,33} Similar to previous results at the HF level,³² the single bond is sensitive to the electrostatic and Pauli exchange interactions. Table 1 shows that the positive charge in the methylene group shortens the single bond (in the allyl cation) by about 0.02 Å, whereas the negative charge lengthens the single C sp^2 –C sp^2 bond length (in the allyl anion) by 0.02 Å with the basis sets of 6-31+G(d) and 6-311+G(d,p) but essentially maintains the bond length unchanged with the cc-pVTZ basis set. Comparison with our previous BLW results at the HF level³² indicates that the electron correlation increases the resonance energy values, particularly in the allyl cation. For instance, the ARE for the allyl cation and anion are 36.6 and 38.1 kcal/mol at the HF level with the 6-311+G(d,p) basis set, but the values are 48.8 and 41.9 kcal/mol at the DFT level with the same basis set. However, the current BLW-DFT calculations once again confirm that the magnitude of resonance in the allyl ions is comparable because the equal distribution of the charge across the system is the primary driving force for the very high and comparable resonance energies in the allyl ions. For the neutral allyl radical, the resonance stabilization is much lower than its ionic counterparts and its resonance energy is about half of those in the allyl ions.

It is also interesting to note that the rigid methylene rotation barriers at the B3LYP/6-311+G(d,p) level are 20.1, 38.4, and 31.1 kcal/mol for the allyl radical, cation and anion, respectively. Although these barriers are in qualitative agreement with the

SCHEME 1

resonance energies, the hyperconjugation effect in the rotated structures stabilizes the systems and makes the final rotation barriers much lower than their respective resonance energies in the planar structures. In other words, the correlation between the rotation barriers and resonance energies, which can be found in many systems including the current allyl systems, is mostly due to the fact that the resonance energies in planar structures are much larger than other factors such as the steric repulsion change in the rotation process and the hyperconjugation stabilization in the rotated structures.

3.2. π -Cation Interactions between Cations and Benzene.

As a pilot test for intermolecular interactions, we studied a kind of extremely strong noncovalent interaction, namely π -cation interaction, which even can compete with full aqueous solvation in binding cations. π -cation interaction plays a key role in biological recognition,^{62,63} where cations such as simple Na⁺ or complex acetylcholine (ACh) bind aromatic components from the amino acids Phe, Tyr, and Trp. The elucidation of the nature of this specific interaction will be especially helpful for the understanding of the mechanisms of enzymatic catalysis and ion channels.

We choose benzene as the π aromatic system to interact with cations. Although benzene is a nonpolar molecule, it has a quadrupole moment, and Dougherty^{63,64} assumed that the electrostatic interaction between the cation and the quadrupole charge distribution of the aromatic is of prime importance in the π -cation interactions,⁶⁵ whereas additional terms such as induced dipoles, polarizabilities, dispersion forces, and charge transfer should be included to quantitatively model the cation- π interactions. Kollman and co-workers showed the molecular mechanical model with polarizability can model π -cation interaction energies better than two-body additive models.⁶⁶ Using a perturbation approach, Cubero et al. explored the importance of cation \rightarrow aromatic polarization effects on cation- π interactions and found that the polarization energy is 70% of the magnitude of the electrostatic energy at the optimal Na⁺-benzene distance of 2.47 Å.⁶⁷

To elucidate the origin of π -cation forces, we investigated the interactions between a few simple cations ($M^+ = Li^+, Na^+, K^+, NH_4^+$, and $N(CH_3)_4^+$, as shown in Figure 1) and the prototypical aromatic system, benzene, with the energy decomposition scheme based on the BLW method,^{30,48,50,55} where the interaction energy with the basis set superposition error (BSSE) correction is decomposed into Heitler–London energy (ΔE_{HL}), polarization energy (ΔE_{pol}) and charge-transfer energy (ΔE_{CT})

$$\begin{aligned} \Delta E_{\text{int}} &= E(\Psi_{AB}) - E(\Psi_A^0) - E(\Psi_B^0) + \text{BSSE} \\ &= \Delta E_{\text{HL}} + \Delta E_{\text{pol}} + \Delta E_{\text{CT}} \end{aligned} \quad (18)$$

where ΔE_{HL} is the energy change by bringing monomers together without disturbing their individual electron densities, ΔE_{pol} corresponds to the redistribution of electron density within each monomer due to the electric field imposed by the other monomer, and ΔE_{CT} is the stabilization energy due to the penetration of electrons between the monomers. It should be noted that ΔE_{HL} is a sum of electrostatic and Pauli exchange repulsion energies. Because the exchange of electrons is a quantum mechanical effect and classical force field approaches have difficulties formulating the exchange energy separately, here we simply use ΔE_{HL} as the electrostatic energy.

Our test calculations on the interactions between cations and benzene are performed with geometries optimized at the MP2/6-311G** level, and subsequent BLW energy analyses are conducted at the B3LYP/6-311G** level. Table 2 compares

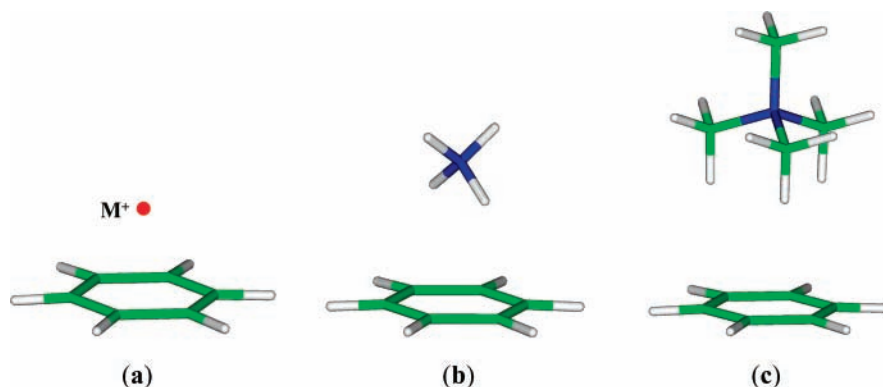


Figure 1. Geometries for the π -cation complexes: (a) $M^+(C_6H_6)$ ($M = Li, Na, K$); (b) $NH_4^+(C_6H_6)$; (c) $N(CH_3)_4^+(C_6H_6)$.

TABLE 2: BLW-DFT Energy Decomposition Analyses on the π -Cation Interactions with the 6-311G(d,p) Basis Set (kcal/mol)^a

| complex | ΔE_{HL} | ΔE_{pol} | ΔE_{CT} | ΔE_{int}^{B3LYP} | ΔE_{int}^{MP2} |
|-----------------------|-----------------|------------------|-----------------|--------------------------|------------------------|
| $Li^+(C_6H_6)$ | -8.3 | -21.9 | -8.9 | -39.1 (-40.2) | -35.8 (-40.1) |
| $Na^+(C_6H_6)$ | -9.6 | -11.6 | -3.0 | -24.2 (-25.4) | -21.8 (-25.2) |
| $K^+(C_6H_6)$ | -5.4 | -7.8 | -3.3 | -16.6 (-17.4) | -17.5 (-20.3) |
| $NH_4^+(C_6H_6)$ | -2.9 | -7.9 | -5.7 | -16.5 (-17.1) | -18.0 (-19.7) |
| $N(CH_3)_4^+(C_6H_6)$ | -0.8 | -2.4 | -2.4 | -5.6 (-6.2) | -9.2 (-11.1) |

^a Data in parentheses are derived without taking the BSSE effect into account.

various energy contributions (electrostatic, polarization, and charge transfer) to the interaction energies ΔE_{int} at the DFT. For comparison, the MP2 interaction energies are also listed to evaluate the residual electron correlation (dispersion energy), which is left out in the DFT calculations. It should be noted that geometries and binding energies for alkali-metal cation complexes with benzene have been extensively studied by Nicholas et al. at various levels,⁶⁸ and our optimizations produced similar results. For instance, the distances between the cation and the center of benzene are 1.88, 2.42, and 2.79 Å for Li^+ , Na^+ , and K^+ at the MP2/6-311G** level, respectively, and data for NH_4^+ and $N(CH_3)_4^+$ are 2.90 and 4.22 Å, respectively. Nicholas et al. also pointed out that MP2 results are well converged with regard to the extent of electron correlation.⁶⁸

As listed in Table 2, the Heitler–London energy decreases in the order $Na^+ > K^+ > NH_4^+ > N(CH_3)_4^+$, in inverse proportionality to the distance between the cation and benzene. But Li^+ is an exception as the Heitler–London energy with benzene is lower than for Na^+ . Further analyses reveal that this abnormality comes from the strong Pauli exchange repulsion due to the short distance between Li^+ and benzene. Overall, ΔE_{HL} accounts for only 21% (Li^+), 40% (Na^+), 33% (K^+), 17% (NH_4^+), and 14% ($N(CH_3)_4^+$) of the interaction energies. This finding is in accord with the failure of previous force field studies based on a pure electrostatic model,⁶⁶ although the latter does provide correct qualitative ordering for the interaction with aromatic compounds.⁶⁴

Notably, our energy decomposition analysis highlights the importance of the polarization effect, which almost solely comes from the aromatic benzene. For the present cation–benzene complexes, the polarization energy contributes about 50% to the interaction energies and decreases in the order $Li^+ > Na^+ > K^+ \approx NH_4^+ > N(CH_3)_4^+$. Like the electrostatic force, the polarization effect decreases with increasing distance between the cation and benzene. Our calculations support previous arguments that the explicit inclusion of polarization in molecular interaction potential is essential to

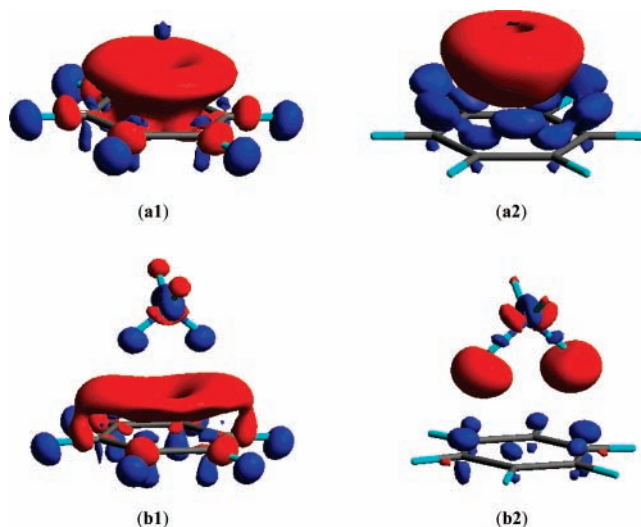


Figure 2. Electron density difference (EDD) maps: (a1) and (b1) show the polarization effect in the $Li^+C_6H_6$ and $NH_4^+C_6H_6$ complexes (isodensity 3×10^{-3} and 2×10^{-3} au, respectively); (a2) and (b2) show the charge-transfer effect in $Li^+C_6H_6$ and $NH_4^+C_6H_6$ (isodensity 1×10^{-3} au).

the modeling of the π -cation interactions.^{66,67,69} Without the inclusion of the polarization effect, even modified OPLS reproducing the quadrupole moment of benzene leads to the Li^+ –benzene complex enthalpy of only -25.3 kcal/mol.⁶⁶ Cubero et al. estimated the polarization stabilization energy -9.9 kcal/mol for the interaction of Na^+ with benzene,⁶⁷ which is in good agreement with our result (-11.6 kcal/mol). To explore the origin of the polarization effect, we evaluated the individual polarization energies of the cation, σ part and π part of benzene and found that the polarization effect is actually dominated by the hybridization of the σ and π parts of benzene.

The polarization of benzene can be visualized by the electron density difference (EDD) between the BLW for the complex and the sum of individual monomers. Figure 2 shows the polarization of benzene in the electrical field of K^+ and NH_4^+ , where the red means the gain of electron density and the blue refers to the loss of electron density. Apparently, the polarization results from the $\sigma \rightarrow \pi^*$ excitation, and the overall effect is the electron density shift from hydrogen (σ orbitals) to carbon (π orbitals). Other cations have the similar effect, and the field effect decreases in the order $Li^+ > Na^+ > K^+ > NH_4^+ > N(CH_3)_4^+$, in accord with the polarization energies.

Kollman and co-workers' nonadditive model⁶⁶ took the polarization effect into account and got the enthalpies close to both experimental and quantum mechanical data. However, the

distance from the cation to the benzene center is noticeably underestimated by about 0.2 Å in all cases. Adjusting the three-body potential may result in good distances, but enthalpies will be underestimated. For the example of $\text{Li}^+(\text{C}_6\text{H}_6)$, the enthalpy is -32.1 kcal/mol when the π -cation distance is 1.9 Å. The dilemma mainly lies in the omission of the charge-transfer effect in their modeling, as Kollman and co-workers assumed. Our analyses endorsed their assumption, and particularly for Li^+ , the charge-transfer stabilizes the $\text{Li}^+(\text{C}_6\text{H}_6)$ complex by 8.9 kcal/mol, which accounts for 23% of the total interaction energy. For other cations, the charge-transfer effect is not as prominent as Li^+ , but still noticeable, particularly for NH_4^+ and $\text{N}(\text{CH}_3)_4^+$. The charge-transfer effect can be visualized by the EDD maps between BLW and DFT wave functions, as shown in Figure 1 for the cases of $\text{Li}^+(\text{C}_6\text{H}_6)$ and $\text{NH}_4^+(\text{C}_6\text{H}_6)$ complexes. The charge transfer mainly occurs from carbon atoms in benzene to Li^+ or the protons in NH_4^+ pointing toward benzene.

The comparison between the DFT and MP2 interaction energies in Table 1 indicates that the counterpoise method⁷⁰ may remarkably overestimate the BSSE correction for MP2 energies.⁷¹ The B3LYP calculations result in a BSSE correction of about 1 kcal/mol, but the correction at the MP2 level is 4.3 kcal/mol for $\text{Li}^+(\text{C}_6\text{H}_6)$ and then decreases with the increasing π -cation distance (or the weakening of the π -cation interaction). However, we still can envision that the dispersion energy plays a noticeable role in the interactions at least between K^+ , NH_4^+ , or $\text{N}(\text{CH}_3)_4^+$ and benzene.

3.3. Charge Transfer in the Solvation of $\text{Me}_n\text{NH}_{4-n}^+$ ($n = 0-3$). Because most chemical reactions and biological processes occur in solution, the simulation of solvent effects has been one of the most active research fields in computational chemistry and significant progresses have been made in both implicit and explicit solvation models.⁷²⁻⁷⁴ In implicit solvation models, a polarizable solvent is efficiently treated as a continuous homogeneous dielectric,⁷² but the strong and specific solute-solvent interactions, e.g., hydrogen bonding, which is a directional short-range force, are not completely accounted for. In explicit solvation models, solvent molecules are usually defined explicitly at the molecular mechanical (MM) level, and the solute is at either the same MM level or at the more advanced quantum mechanical (QM) level. A critical component in the explicit solvation models is the intermolecular potential function that describes intermolecular interactions in the condensed phase, and ultimately determines the success of computer simulations.⁷⁵ With the recognition of the importance of the solvent polarization effect in solute-solvent interactions, polarizable force fields where explicit polarization terms are added in the potential energy function have been proposed and developed.⁷⁶ However, there have been controversies over the magnitude of charge transfer between solute and solvent molecules.^{48,77,78} We note that the controversies mostly originate from the various definitions of the charge-transfer energy term in numerous energy decomposition schemes.⁷⁹ The uniqueness of our BLW energy decomposition method lies in the construction of an intermediate diabatic state where charge transfer is deactivated and the corresponding wavefunction is self-consistently optimized. Using such a diabatic state as a reference, both the polarization and charge-transfer effects can be distinctly differentiated.

Most recently, we performed combined QM/MM simulations on the solvation of two simple ionic systems, acetate and methylammonium, in a water box, followed by BLW energy decomposition analyses at the HF level on a few randomly selected configurations where the first and second hydration

TABLE 3: BLW-DFT Energy Decomposition Analyses on the Interaction between $\text{Me}_n\text{NH}_{4-n}^+$ and Water with the 6-311+G(d,p) Basis Set (kcal/mol)^a

| complex | ΔE_{HL} | ΔE_{pol} | ΔE_{CT} | $\Delta E_{\text{int}}^{\text{B3LYP}}$ | $\Delta E_{\text{int}}^{\text{MP2}}$ |
|--|------------------------|-------------------------|------------------------|--|--------------------------------------|
| $\text{NH}_4^+(\text{H}_2\text{O})_4$ | -50.8 | -11.5 | -7.7 | -70.0 (-74.0) | -67.5 (-74.5) |
| $\text{MeNH}_3^+(\text{H}_2\text{O})_3$ | -34.1 | -9.4 | -6.6 | -50.1 (-53.2) | -48.7 (-54.4) |
| $\text{Me}_2\text{NH}_2^+(\text{H}_2\text{O})_2$ | -20.2 | -6.8 | -5.2 | -32.2 (-34.2) | -31.6 (-35.7) |
| $\text{Me}_3\text{NH}^+(\text{H}_2\text{O})$ | -8.8 | -3.7 | -3.1 | -15.6 (-16.6) | -15.5 (-17.8) |

^a Data in parentheses are derived without taking the BSSE effect into account.

shells of water molecules are included in the QM part. We found that the charge-transfer term only makes a small fraction of the total solute-solvent interaction energy.⁴⁸ However, we note that the force field used in the simulation is nonpolarizable and as a consequence, the distance between the solute and the first hydration shell may be more or less lengthened as the short-range polarization interaction has been diluted to the long-range electrostatic interaction by adjusting the atomic partial charges in nonpolarizable force fields. For instance, the radial distribution function showed the peak of the average acetate oxygen or methylammonium nitrogen and water oxygen in the first hydration shell at 2.95 or 2.85 Å,⁴⁸ compared with 2.75 and 2.85 Å from Car-Parrinello simulations with plane-wavefunction DFT by Peraro et al.⁷⁸ Because the charge transfer is very sensitive to the distance and increases in an exponential pattern,³⁵ it would be of general interests to derive the solute-solvent configurations at the ab initio level.

Here we estimated the charge-transfer effect in the solvation of ammonium and its methyl substitutes with supermolecular models $\text{Me}_n\text{NH}_{4-n}^+\cdots(\text{H}_2\text{O})_{4-n}$ ($n = 0-3$),⁸⁰ where each N-H group forms a hydrogen bond with a water molecule. The BLW-DFT calculations and analyses are conducted at the geometries optimized at the MP2/6-311+G(d,p) level. Results are summarized in Table 3, where the MP2 interaction energies are also listed for comparison.

Due to the very small size of solvent molecules in the present models, the total solute-solvent interaction energies are much lower than the true cases. For instance, the QM/MM data for the solvation of MeNH_3^+ is -122.0 kcal/mol,³⁵ whereas the present model gave only -50.1 kcal/mol. We believe the difference mostly comes from the long-range electrostatic interactions, plus a small portion from the solvent polarization. With the reduction of the water molecule number in the models, the solute-solvent interaction energy decreases dramatically from -70.0 kcal/mol in $\text{NH}_4^+(\text{H}_2\text{O})_4$ to only -15.6 kcal/mol $\text{Me}_3\text{NH}^+(\text{H}_2\text{O})$, indicating the inappropriateness of these models to study the solvation of ions. However, we note that our objective here is to evaluate the contribution from the charge-transfer effect to the solute-solvent interactions, rather than get accurate solvation energies. The current calculations do confirm that the permanent electrostatic energy dominates the solute-solvent interactions, and polarization effect plays the secondary role. The charge-transfer energy is comparable in magnitude with the polarization effect; nevertheless, we expect that the inclusion of more water molecules in models will remarkably increase both the Heitler-London and polarization energies but retain the charge-transfer energy at the current level. More extensive studies currently are still under way.

If we focus on individual hydrogen bonds in the four systems, the charge-transfer energy for each N-H \cdots OH₂ bond is -1.9 , -2.2 , -2.6 , and -3.1 kcal/mol, in good correlation with the hydrogen bond distance $R_{\text{N-O}} = 2.860$, 2.840, 2.818, and 2.792 Å in the four optimal models. Similar to previous work, we also probed individual polarization contributions from the solute

TABLE 4: Individual Polarization Energies (kcal/mol)

| complex | $\Delta E_{\text{pol}} (\text{M}^+)$ | $\Delta E_{\text{pol}} (\text{water})$ |
|--|--------------------------------------|--|
| $\text{NH}_4^+(\text{H}_2\text{O})_4$ | -0.4 | -11.1 |
| $\text{MeNH}_3^+(\text{H}_2\text{O})_3$ | -1.3 | -7.7 |
| $\text{Me}_2\text{NH}_2^+(\text{H}_2\text{O})_2$ | -1.4 | -4.9 |
| $\text{Me}_3\text{NH}^+(\text{H}_2\text{O})$ | -0.9 | -2.4 |

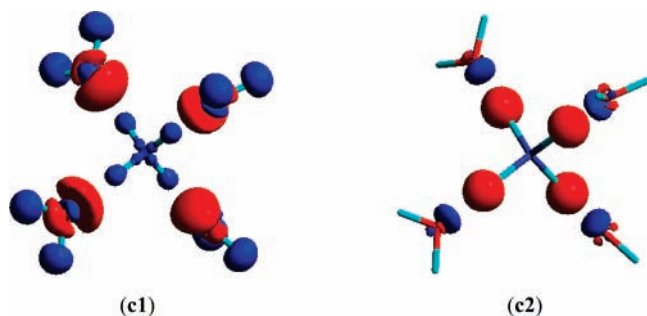


Figure 3. Electron density difference (EDD) maps for the $\text{NH}_4^+(\text{H}_2\text{O})_4$ cluster model showing (c1) the polarization effect (isodensity 3×10^{-3}) and (c2) the charge-transfer effect (isodensity 2×10^{-1} au).

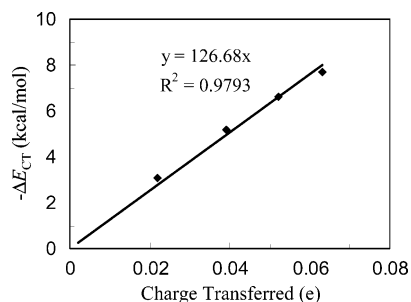


Figure 4. Correlation between the charge-transfer stabilization energy and the amount of NPA charge transferred from water molecules to the cations.

and solvent separately, and Table 4 lists the polarization energy of the solute by the solvent charge density in the absence of the solute, and the polarization energy of the solvent by the solute permanent (gas phase) charge density. Due to the coupling effect, the sum of individual polarization energies is slightly lower than the total polarization energy listed in Table 3. But Table 4 demonstrates that the solvent polarization effect is far more significant than the solute polarization effect. Figure 3-(c1) plots that the solvent polarization shifts the electron density from the O–H σ bond to the oxygen side, and this shifted electron density will be subsequently donated to the protons in ammonium ion as manifested by Figure 3 (c2).

We can further conduct population analyses on the electron densities derived by both the conventional DFT and BLW-DFT computations and take the differences as the charge transferred between the solute and water. Table 5 compiled the amount of charge transferred in the $\text{Me}_n\text{NH}_{4-n}^+\cdots(\text{H}_2\text{O})_{4-n}$ complexes based on three population analysis schemes, namely Mulliken, Löwdin, and natural population analysis (NPA).⁸¹ We can see the latter two derive very similar results, and excellent correlation between the electron-transfer energies (Table 3) and population analyses can be found, as shown in Figure 4.

4. Summary and Prospect

Due to its intuitive concepts and bonding pictures, VB theory has been attractive to chemists. Unfortunately, due to the high computational demands, ab initio VB methods severely lag behind MO-based methods although significant renewed endeavors and progresses have been observed lately.^{9,12,38} Instead,

TABLE 5: Amount of Electrons Transferred from Water to $\text{Me}_n\text{NH}_{4-n}^+$ Based on Various Population Analysis Schemes

| complex | Mulliken | Löwdin | NPA |
|--|----------|--------|-------|
| $\text{NH}_4^+(\text{H}_2\text{O})_4$ | 0.041 | 0.060 | 0.063 |
| $\text{MeNH}_3^+(\text{H}_2\text{O})_3$ | 0.050 | 0.053 | 0.052 |
| $\text{Me}_2\text{NH}_2^+(\text{H}_2\text{O})_2$ | 0.048 | 0.043 | 0.039 |
| $\text{Me}_3\text{NH}^+(\text{H}_2\text{O})$ | 0.033 | 0.021 | 0.022 |

various empirical and semiempirical VB approaches have been proposed and extensively applied to the elucidation of the correlations between molecular structures and properties, and the studies of chemical reactions in solution and enzyme.^{10,15–22} Our proposed BLW method takes advantage of both the MO and VB theories and is an ab initio VB-like method with the high efficiency of the HF and DFT methods. Because the BLW method is based on a single Slater determinant, its extension to the DFT level can effectively take electron correlation into account. Although the BLW method is not general but restricted to specific cases, these cases are sufficiently numerous and interesting to make the method highly useful. Test applications show that the BLW-DFT method has negligible basis set dependency and thus can be reliably used to study the intramolecular electron delocalization and the intermolecular charge-transfer effect.

Because diabatic states can be defined by BLWs at the ab initio level individually, the important off diagonal matrix element H_{AB} can be subsequently computed and its dependency on the environment can also be examined. As an adiabatic state is a combination of two or more diabatic states, BLW-based two-state (or multistate) approaches can be developed. This kind of two-state approach can study not only the chemical reactions as done by EVB but also the electron-transfer processes and thus establish the qualitative Marcus–Hush model at the quantitative level. The combination of the BLW method with MD simulation codes can further allow the combined QM-(BLW)/MM approach to study the solvent reorganization effect, which is critical in electron-transfer theory.^{74,82}

Acknowledgment. This work is supported by the Keck foundation, the National Institute of Health (NIH), and Western Michigan University.

References and Notes

- (1) Lewis, G. N. *J. Am. Chem. Soc.* **1916**, *38*, 762.
- (2) *90 Years of Chemical Bonding*; Frenking, G., Shaik, S., Eds.; Journal of Computational Chemistry; Wiley: New York, 2007; Vol. 28, No. 1, pp 1 (special issue).
- (3) Heitler, W.; London, F. Z. *Phys.* **1927**, *44*, 455.
- (4) Slater, J. C. *Phys. Rev.* **1931**, *37*, 481. Slater, J. C. *Phys. Rev.* **1931**, *37*, 1109. Pauling, L. *J. Am. Chem. Soc.* **1931**, *53*, 3225. Pauling, L. *J. Am. Chem. Soc.* **1931**, *53*, 1367.
- (5) Pauling, L. C. *The Nature of the Chemical Bond*, 3rd ed.; Cornell University Press: Ithaca, NY, 1960.
- (6) Wheland, G. W. *Resonance in Organic Chemistry*; Wiley & Sons: New York, 1955.
- (7) Foster, J. M.; Boys, S. F. *Rev. Mod. Phys.* **1960**, *32*, 300. Edmiston, C.; Ruedenberg, K. *Rev. Mol. Phys.* **1963**, *35*, 457. Pipek, J.; Mezey, P. G. *J. Chem. Phys.* **1989**, *90*, 4916. Foster, J. P.; Weinhold, F. *J. Am. Chem. Soc.* **1980**, *102*, 7211. Reed, A. E.; Curtiss, L. A.; Weinhold, F. *Chem. Rev.* **1988**, *88*, 899.
- (8) *Valence Bond Theory*; Cooper, D. L., Ed.; Elsevier: Amsterdam, 2002. Zhang, Q.; Li, X. *J. Mol. Struct.* **1989**, *189*, 413. Hiberty, P. C. *THEOCHEM* **1997**, *398–399*, 35. Mcweeny, R. *Int. J. Quantum Chem.* **1999**, *74*, 87.
- (9) Gallup, G. A.; Vance, R. L.; Collins, J. R.; Norbeck, J. M. *Adv. Quantum Chem.* **1982**, *16*, 229. Cooper, D. L.; Gerratt, J.; Raimondi, M. *Nature* **1986**, *323*, 699. Cooper, D. L.; Gerratt, J.; Raimondi, M. *Chem. Rev.* **1991**, *91*, 929. Thorsteinsson, T.; Cooper, D. L. *J. Math. Chem.* **1998**, *23*, 105. Wu, W.; Shaik, S. *Chem. Phys. Lett.* **1999**, *301*, 37. Dijkstra, F.; van Lenthe, J. H. *J. Chem. Phys.* **2000**, *113*, 2100. Li, J.; McWeeny, R. *Int. J. Quantum Chem.* **2002**, *89*, 208.

- (10) Shaik, S.; Shurki, A. *Angew. Chem., Int. Ed.* **1999**, *38*, 586.
- (11) Hiberty, P. C.; Shaik, S. *J. Comput. Chem.* **2007**, *28*, 137.
- (12) Wu, W.; Wu, A.; Mo, Y.; Lin, M.; Zhang, Q. *Int. J. Quantum Chem.* **1998**, *67*, 287. Wu, W.; Song, L.; Mo, Y.; Zhang, Q. XIAMEN-99: An ab initio spin-free valence bond (VB) program; Xiamen University: Xiamen, 2000.
- (13) Song, L.; Mo, Y.; Zhang, Q.; Wu, W. *J. Comput. Chem.* **2005**, *26*, 514.
- (14) Truhlar, D. G. *J. Comput. Chem.* **2007**, *28*, 73.
- (15) Warshel, A.; Weiss, R. M. *J. Am. Chem. Soc.* **1980**, *102*, 6218. Åqvist, J.; Warshel, A. *Chem. Rev.* **1993**, *93*, 2523.
- (16) Warshel, A. *Computer Simulation of Chemical Reactions in Enzymes and Solutions*; John Wiley & Sons: New York, 1991.
- (17) Chang, Y.-T.; Miller, W. H. *J. Phys. Chem.* **1990**, *94*, 5884.
- (18) Bernardi, F.; Olivucci, M.; Robb, M. A. *J. Am. Chem. Soc.* **1992**, *114*, 1606. Chen, G.; Lu, D.; Goddard, W. A., III. *J. Chem. Phys.* **1994**, *101*, 5860. Lu, D.; Chen, G.; Perry, J. W.; Goddard, W. A., III. *J. Am. Chem. Soc.* **1994**, *116*, 10679. Shaik, S.; Hiberty, P. C. *Adv. Quantum Chem.* **1995**, *26*, 99. Cullen, J. M. *Int. J. Quantum Chem.* **1995**, *56*, 97. Grochowski, P.; Lesyng, B.; Bala, P.; McCammon, J. A. *Int. J. Quantum Chem.* **1998**, *60*, 1143. Lobaugh, J.; Voth, G. A. *J. Chem. Phys.* **1996**, *104*, 2056. Bala, P.; Grochowski, P.; Lesyng, B.; McCammon, J. A. *J. Am. Chem. Soc.* **1996**, *100*, 2535. Thompson, W. H.; Blanchard-Desce, M.; Hynes, J. T. *J. Phys. Chem. A* **1998**, *102*, 7712. Thompson, W. H.; Blanchard-Desce, M.; Alain, V.; Muller, J.; Fort, A.; Barzoukas, M.; Hynes, J. T. *J. Phys. Chem. A* **1999**, *103*, 3766. Sagnella, D. E.; Tuckerman, M. E. *J. Chem. Phys.* **1998**, *108*, 2073. Day, T. J. F.; Soudackov, A. V.; Cuma, M.; Schmitt, U. W.; Voth, G. A. *J. Chem. Phys.* **2002**, *117*, 5839. Valone, S. M.; Atlas, S. R. *J. Chem. Phys.* **2004**, *120*, 7262. Shurki, A.; Crown, H. A. *J. Phys. Chem. B* **2005**, *109*, 23638. Maupin, C. M.; Wong, K. F.; Soudackov, A. V.; Kim, S.; Voth, G. A. *J. Phys. Chem. A* **2006**, *110*, 631. Bearpark, M. J.; Boggio-Pasqua, M.; Robb, M. A.; Ogliaro, F. *Theor. Chem. Acc.* **2006**, *116*, 670.
- (19) Schmitt, U. W.; Voth, G. A. *J. Phys. Chem. B* **1998**, *102*, 5547. Schmitt, U. W.; Voth, G. A. *J. Chem. Phys.* **1999**, *111*, 9361. Kim, Y.; Corchado, J. C.; Villà, J.; Xing, J.; Truhlar, D. G. *J. Chem. Phys.* **2000**, *112*, 2718. Albu, T. V.; Corchado, J. C.; Truhlar, D. G. *J. Phys. Chem. A* **2001**, *105*, 8465.
- (20) Vuilleumier, R.; Borgis, D. *Isr. J. Chem.* **1999**, *39*, 457. Lin, H.; Zhao, Y.; Tishchenko, O.; Truhlar, D. G. *J. Chem. Theory Comput.* **2006**, *2*, 1237.
- (21) Schlegel, H. B.; Sonnenberg, J. L. *J. Chem. Theory Comput.* **2006**, *2*, 905.
- (22) Linares, M.; Braida, B.; Humbel, S. *J. Phys. Chem. A* **2006**, *110*, 2505.
- (23) Vuilleumier, R.; Borgis, D. *Chem. Phys. Lett.* **1998**, *284*, 71.
- (24) Marcus, R. A. *J. Chem. Phys.* **1956**, *24*, 966. Marcus, R. A. *Annu. Rev. Phys. Chem.* **1964**, *15*, 155. Hush, N. S. *Electrochim. Acta* **1968**, *13*, 1005.
- (25) Marcus, R. A.; Sutin, N. *Biochim. Biophys. Acta* **1985**, *811*, 265. Mulliken, R. S. *J. Am. Chem. Soc.* **1952**, *74*, 811. Logan, J.; Newton, M. D. *J. Chem. Phys.* **1983**, *78*, 4086. Ohta, K.; Closs, G. L.; Morokuma, K.; Green, N. J. *J. Am. Chem. Soc.* **1986**, *108*, 1319. Cave, R. J.; Baxter, D. V.; Goddard, W. A., III; Baldeschwieler, J. D. *J. Chem. Phys.* **1987**, *87*, 926. Farazdel, A.; Dupuis, M.; Clementi, E.; Aviram, A. *J. Am. Chem. Soc.* **1990**, *112*, 4206. Farazdel, A.; Dupuis, M. *J. Comput. Chem.* **1991**, *12*, 276. Newton, M. D. *Chem. Rev.* **1991**, *91*, 767. Cave, R. J.; Newton, M. D. *J. Chem. Phys.* **1997**, *106*, 9213. Rust, M.; Lappe, J.; Cave, R. J. *J. Phys. Chem. A* **2002**, *106*, 3930. Voityuk, A. A.; Rösch, N. *J. Chem. Phys.* **2002**, *117*, 5607. Pourtois, G.; Beljonne, D.; Cornil, J.; Ratner, M. A.; Bredas, J. L. *J. Am. Chem. Soc.* **2002**, *124*, 4436. Mo, Y.; Wu, W.; Zhang, Q. *J. Chem. Phys.* **2003**, *119*, 6448. Improta, R.; Barone, V.; Newton, M. D. *Chem. Phys. Chem.* **2006**, *7*, 1211. Prytkova, T. R.; Kurnikov, I. V.; Beratan, D. N. *J. Phys. Chem. B* **2005**, *109*, 1618.
- (26) Hong, G. Y.; Rosta, E.; Warshel, A. *J. Phys. Chem. B* **2006**, *110*, 19570.
- (27) Villa, J.; Bentzien, J.; Gonzalez-Lafont, A.; Lluch, J. M.; Bertran, J.; Warshel, A. *J. Comput. Chem.* **2000**, *21*, 607.
- (28) Goddard, W. A. *J. Phys. Rev.* **1967**, *157*, 73. Bobrowicz, F. W.; Goddard, W. A., III. The self-consistent field equations for generalized valence bond and open-shell Hartree-Fock wave functions. In *Methods of Electronic Structure Theory*; Schaefer, H. F., III, Ed.; Plenum: New York, 1977; pp 79.
- (29) Mo, Y.; Peyerimhoff, S. D. *J. Chem. Phys.* **1998**, *109*, 1687.
- (30) Mo, Y.; Gao, J.; Peyerimhoff, S. D. *J. Chem. Phys.* **2000**, *112*, 5530.
- (31) Mo, Y. *J. Chem. Phys.* **2003**, *119*, 1300.
- (32) Mo, Y. *J. Org. Chem.* **2004**, *69*, 5563.
- (33) Mo, Y.; Schleyer, P. v. R. *Chem. Eur. J.* **2006**, *12*, 2009.
- (34) Mo, Y. *Curr. Org. Chem.* **2006**, *10*, 779.
- (35) Mo, Y.; Song, L.; Wu, W.; Zhang, Q. *J. Am. Chem. Soc.* **2004**, *126*, 3974.
- (36) Kohn, W. *Rev. Mod. Phys.* **1998**, *71*, 1253. Kohn, W.; Sham, L. J. *Phys. Rev.* **1965**, *140*, 1133. Bickelhaupt, F. M.; Baerends, E. J. Kohn-Sham density functional theory: Predicting and understanding chemistry. In *Reviews in Computational Chemistry*; Lipkowitz, K. B., Boyd, D. B., Eds.; Wiley-VCH: New York, 1999; Vol. 15, pp 1. Zhao, Y.; Schultz, N. E.; Truhlar, D. G. *J. Chem. Theory Comput.* **2006**, *2*, 364.
- (37) Schmidt, M. W.; Baldrige, K. K.; Boatz, J. A.; Elbert, S. T.; Gordon, M. S.; Jensen, J. J.; Koseki, S.; Matsunaga, N.; Nguyen, K. A.; Su, S.; Windus, T. L.; Dupuis, M.; Montgomery, J. A. *J. Comput. Chem.* **1993**, *14*, 1347.
- (38) Wu, W.; Mo, Y.; Cao, Z.; Zhang, Q. A spin-free approach for valence bond theory and its applications. In *Valence Bond Theory*; Cooper, D. L., Ed.; Elsevier: Amsterdam, 2002; Vol. 10, pp 143.
- (39) Mulliken, R. S.; Parr, R. G. *J. Chem. Phys.* **1951**, *19*, 1271.
- (40) Sovers, O. J.; Kern, C. W.; Pitzer, R. M.; Karplus, M. *J. Chem. Phys.* **1968**, *49*, 2592.
- (41) Kollmar, H. *J. Am. Chem. Soc.* **1979**, *101*, 4832.
- (42) Daudy, J. P.; Trinquier, G.; Barthelat, J. C.; Malrieu, J. P. *Tetrahedron* **1980**, *36*, 3399.
- (43) Hush, N. S. *Trans. Faraday Soc.* **1961**, *57*, 557.
- (44) Gianinetti, E.; Raimondi, E. *Int. J. Quantum Chem.* **1996**, *60*, 157. Gianinetti, E.; Vandoni, I.; Famulari, A.; Raimondi, M. *Adv. Quantum Chem.* **1998**, *31*, 251. Famulari, A.; Specchio, R.; Gianinetti, E.; Raimondi, M. Ab Initio computational approaches to weakly interacting systems in the framework of the valence bond theory: from small to large van der Waals molecules. In *Valence Bond Theory*; Cooper, D. L., Ed.; Elsevier: Amsterdam, 2002; Vol. 10, pp 313.
- (45) Famulari, A.; Gianinetti, E.; Raimondi, M.; Sironi, M. *Int. J. Quantum Chem.* **1998**, *69*, 151.
- (46) Mo, Y.; Wu, W.; Song, L.; Lin, M.; Zhang, Q.; Gao, J. *Angew. Chem., Int. Ed.* **2004**, *43*, 1986. Mo, Y.; Gao, J. *Acc. Chem. Res.* **2007**, *40*, 113.
- (47) Mo, Y.; Subramanian, G.; Ferguson, D. M.; Gao, J. *J. Am. Chem. Soc.* **2002**, *124*, 4832.
- (48) Mo, Y.; Gao, J. *J. Phys. Chem. B* **2006**, *110*, 2976.
- (49) Mo, Y.; Schleyer, P. v. R.; Wu, W.; Lin, M.; Zhang, Q.; Gao, J. *J. Phys. Chem. A* **2003**, *107*, 10011.
- (50) Mo, Y.; Gao, J. *J. Phys. Chem. A* **2001**, *105*, 6530.
- (51) Parr, R. G.; Yang, W. *Density-Functional Theory of Atoms and Molecules*; Oxford University Press: New York, 1989. *Progress in Density Functional Theory*; Frenking, G., Ed.; Journal of Computational Chemistry; Wiley: New York, 1999; Vol. 20, p 1 (special issue).
- (52) Baer, R.; Neuhauser, D. *Phys. Rev. Lett.* **2005**, *94*, Art. No. 043002. Zhao, Y.; Truhlar, D. G. *J. Phys. Chem. A* **2006**, *110*, 10478. Champagne, B.; Bulat, F. A.; Yang, W. T.; Bonness, S.; Kirtman, B. *J. Chem. Phys.* **2006**, *125*, Art. No. 194114.
- (53) Zimmerli, U.; Parrinello, M.; Koumoutsakos, P. *J. Chem. Phys.* **2004**, *120*, 2693. Becke, A. D.; Johnson, E. R. *J. Chem. Phys.* **2005**, *122*, Art. No. 154104. Grimme, S. *J. Comput. Chem.* **2006**, *27*, 1787.
- (54) Pulay, P. *Chem. Phys. Lett.* **1982**, *73*, 393.
- (55) Mo, Y. *J. Mol. Mod.* **2006**, *12*, 665.
- (56) Wheland, G. W. *The Theory of Resonance*; John Wiley & Sons: New York, 1944.
- (57) Hrovat, D. A.; Borden, W. T. *J. Phys. Chem.* **1994**, *98*, 10460. Glendenning, E. D.; Hrabal, J. A. *J. Am. Chem. Soc.* **1997**, *119*, 12940. Kemnitz, C. R.; Loewen, M. J. *J. Am. Chem. Soc.* **2007**, *129*, 2521.
- (58) Wiberg, K. B.; Breneman, C. M.; LePage, T. J. *J. Am. Chem. Soc.* **1990**, *112*, 61.
- (59) Gobbi, A.; Frenking, G. *J. Am. Chem. Soc.* **1994**, *116*, 9275.
- (60) Mo, Y.; Lin, Z.; Wu, W.; Zhang, Q. *J. Phys. Chem.* **1996**, *100*, 6469.
- (61) Barbour, J. B.; Karty, J. M. *J. Org. Chem.* **2004**, *69*, 648.
- (62) Sussman, J. L.; Harel, M.; Frolow, F.; Oefner, C.; Goldman, A.; Tokar, L.; Silman, I. *Science* **1991**, *253*, 872. Ma, J. C.; Dougherty, D. A. *Chem. Rev.* **1997**, *97*, 1303. Gallivan, J. P.; Dougherty, D. A. *Proc. Natl. Acad. Sci. U.S.A.* **1999**, *96*, 9459. Siu, F. M.; Ma, N. L.; Tsang, C. W. *Chem. Eur. J.* **2004**, *10*, Hughes, R. M.; Waters, M. L. *J. Am. Chem. Soc.* **2006**, *128*, 13586.
- (63) Dougherty, D. A. *Science* **1996**, *271*, 163.
- (64) Mecozzi, S.; West, A. P.; Dougherty, D. A. *J. Am. Chem. Soc.* **1996**, *118*, 2307.
- (65) Gentle, I. R.; Ritchie, G. L. D. *J. Phys. Chem.* **1989**, *93*, 7740.
- (66) Caldwell, J. W.; Kollman, P. A. *J. Am. Soc. Chem.* **1995**, *117*, 4177.
- (67) Cubero, E.; Luque, F. J.; Orozco, M. *Proc. Natl. Acad. Sci. U.S.A.* **1998**, *95*, 5976.
- (68) Nicholas, J. B.; Hay, B. P.; Dixon, D. A. *J. Phys. Chem. A* **1999**, *103*, 1394.
- (69) Eriksson, M. A. L.; Morgantini, P. Y.; Kollman, P. A. *J. Phys. Chem. B* **1999**, *103*, 4474. Cubero, E.; Orozco, M.; Luque, F. J. *J. Phys. Chem. A* **1999**, *103*, 315.
- (70) Boys, S. F.; Bernardi, F. *Mol. Phys.* **1970**, *19*, 553.
- (71) Kim, K. S.; Lee, J. Y.; Lee, S. J.; Ha, T.-K.; Kim, D. H. *J. Am. Chem. Soc.* **1994**, *116*, 7399.
- (72) Tomasi, J.; Persico, M. *Chem. Rev.* **1994**, *94*, 2027. Cramer, C. J.; Truhlar, D. G. *Chem. Rev.* **1999**, *99*, 2161.

(73) Jorgensen, W. L. *Acc. Chem. Res.* **1989**, *22*, 184. van Gunsteren, W. F.; Berendsen, H. J. C. *Angew. Chem., Int. Ed.* **1990**, *29*, 992. Amovilli, C.; Barone, V.; Cammi, R.; Cancès, E.; Cossi, M.; Mennucci, B.; Pomelli, C. S.; Tomasi, J. *Adv. Quantum Chem.* **1999**, *32*, 227. Orozco, M.; Luque, F. J. *Chem. Rev.* **2003**, *100*, 4187.

(74) Gao, J.; Garcia-Viloca, M.; Poulsen, T. D.; Mo, Y. *Adv. Phys. Org. Chem.* **2003**, *38*, 161.

(75) MacKerell, A. D.; Bashford, D.; Bellott, M.; Dunbrack, R. L.; Evanseck, J. D.; Field, M. J.; Fischer, S.; Gao, J.; Guo, H.; Ha, S.; Joseph-McCarthy, D.; Kuchnir, L.; Kuczera, K.; Lau, F. T. K.; Matto, C.; Michnick, S.; Ngo, T.; Nguyen, D. T.; Prodhom, B.; Eeher, W. E.; Roux, B.; Schlenkrich, M.; Smith, J. C.; Stobe, R.; Straub, J.; Watanabe, M.; Wiorkiewicz-Kuczera, J.; Yin, D.; Karplus, M. *J. Phys. Chem. B* **1998**, *102*, 3586. Kollman, P. A.; Merz, K. M. *Acc. Chem. Res.* **1990**, *23*, 246. Kaminski, G. A.; Friesner, R. A.; Tirado-Rives, J.; Jorgensen, W. L. *J. Phys. Chem. B* **2001**, *105*, 6474.

(76) Gao, J. *J. Comput. Chem.* **1997**, *18*, 1062. Rick, S. W.; Stuart, S. J.; Berne, B. J. *J. Chem. Phys.* **1994**, *101*, 6141. Thompson, M. A.; Schenter, G. K. *J. Phys. Chem.* **1995**, *99*, 6374. Banks, J. L.; Kaminski, G. A.; Zhou, R.; Mainz, D. T.; Berne, B. J.; Friesner, R. A. *J. Chem. Phys.* **1999**, *110*, 741. Mahoney, M. W.; Jorgensen, W. L. *J. Chem. Phys.* **2001**, *114*, 9337. Lamoureux, G.; Roux, B. *J. Chem. Phys.* **2003**, *119*, 3025. Curutchet, C.;

Bofill, J. M.; Hernandez, B.; Orozco, M.; Luque, F. J. *J. Comput. Chem.* **2003**, *24*, 1263. Wu, Y.; Yang, Z. *J. Phys. Chem. A* **2004**, *108*, 7563.

(77) Thompson, W. H.; Hynes, J. T. *J. Am. Chem. Soc.* **2000**, *122*, 6278. Robertson, W. H.; Johnson, M. A. *Annu. Rev. Phys. Chem.* **2003**, *54*, 173. Nadig, G.; Van Zant, L. C.; Dixon, S. L.; Merz, K. M., Jr. *J. Am. Chem. Soc.* **1998**, *120*, 5593. van der Vaart, A.; Merz, K. M., Jr. *J. Am. Chem. Soc.* **1999**, *121*, 9182.

(78) Dal Peraro, M.; Raugei, S.; Carloni, P.; Klein, M. L. *Chem. Phys. Chem.* **2005**, *6*, 1715.

(79) Kitaura, K.; Morokuma, K. *Int. J. Quantum Chem.* **1976**, *10*, 325. Stevens, W. J.; Fink, W. H. *Chem. Phys. Lett.* **1987**, *139*, 15. Gutowski, M.; Piel, L. *Mol. Phys.* **1988**, *64*, 337. Cybulski, S. M.; Scheiner, S. *Chem. Phys. Lett.* **1990**, *166*, 57. Moszynski, R.; Heijmen, T. G. A.; Jeziorski, B. *Mol. Phys.* **1994**, *88*, 741. Glendening, E. D.; Streitwieser, A. *J. Chem. Phys.* **1994**, *100*, 2900. van der Vaart, A.; Merz, K. M., Jr. *J. Phys. Chem. A* **1999**, *103*, 3321.

(80) Cao, Z.; Lin, M.; Zhang, Q.; Mo, Y. *J. Phys. Chem. A* **2004**, *108*, 4277.

(81) Löwdin, P.-O. *Adv. Quantum Chem.* **1970**, *5*, 185. Reed, A. E.; Weinhold, F. *Isr. J. Chem.* **1991**, *31*, 277.

(82) Mo, Y.; Gao, J. *J. Comput. Chem.* **2000**, *21*, 1458. Mo, Y.; Gao, J. *J. Phys. Chem. A* **2000**, *104*, 3012.